

## Anti-Strike Capability of Steel-Fiber Reactive Powder Concrete

Fan Pengxian\*, Wang Mingyang, and Song Chunming

*PLA University of Science and Technology, Nanjing-210 007, China*

*\*E-mail: fan-px@139.com*

### ABSTRACT

Penetration and contact explosion tests on reactive powder concrete (RPC) containing 5 per cent steel-fiber were carried out to investigate the anti-strike capability of steel-fiber reactive powder concrete (SFRPC). The penetration tests consisted of two sample groups corresponding to hit speeds 308 m/s - 582 m/s and 808 m/s - 887 m/s, respectively. The contact explosion tests were carried out in an explosion test pit using TNT with charges in the range 0.5 kg - 3.0 kg. The tests results show that the anti-strike capability of SFRPC targets is much better than ordinary C30 concrete. The penetration depths of the SFRPC targets were less than half those evaluated values of the C30 concrete targets. The areas of the blasting funnels and the explosion cavity radii in the SFRPC plates are also much less than the calculated results in ordinary C30 concrete, being about one quarter of those of the latter.

**Keywords:** Destructive testing, steel-fiber reactive powder concrete, penetration, contact explosion

### 1. INTRODUCTION

Due to a rapid development in precision-guided and penetrating weapons, existing protective engineering face a great challenge and severe threat. Generally, there are two methods used to improve the performance of protective engineering structures against attacks. One is to seek advanced structural systems to mitigate and/or disperse the energy of the impact (penetration or explosion), and the other is to apply new high-performance materials to enhance the anti-strike capability of the structure.

In recent decades, steel-fiber high-strength concrete has become a popular material in structural engineering suitable for possible exposure to accidental explosions and other harsh environments<sup>1</sup>. Reactive powder concrete (RPC) is a kind of advanced cement-based material, originally developed in the early 1990s. RPC possesses ultra-high static/dynamic strength, high fracture capacity, low shrinkage, and excellent durability under severe conditions<sup>2-4</sup>. The addition of steel fiber further improves the dynamic properties of the concrete<sup>5,6</sup>. However, the high cost and complex fabrication technique required to make SFRPC severely limits its commercial development and application in civil engineering. However, in the construction of important protective engineering structures for military purpose, anti-strike capability has priority over cost. Thus, SFRPC is a commendable choice to use as a substitute for ordinary concrete in the construction of such protective structures.

As the application and demand for SFRPC increased, several experimental studies were conducted to investigate

its static and dynamic properties and to develop new rules for its proper design<sup>7,8</sup>. The test results showed that SFRPC demonstrates high-quality toughness and high residual strength even after cracks have appeared. SFRPC possesses most of the properties required for protective engineering applications. However, there are only a few reports published in the literature devoted to investigating the anti-penetration or anti-explosion performance of SFRPC structures. To investigate the anti-strike capability of SFRPC, a group of tests on SFRPC under penetration and contact explosion conditions have been carried out.

### 2. EXPERIMENTAL METHODS

#### 2.1 Materials

The SFRPC material used in this study is developed by State Key Laboratory of Disaster Prevention and Mitigation of Explosion and Impact, China. Fine aggregate was used to improve uniformity and the best particle size gradation and steam curing techniques were adopted to improve compaction and microstructure. A series of static and dynamic tests, including concrete mixing tests, maintenance tests, uniaxial compression tests, tensile tests, impact tests and mass concrete construction tests, were conducted to investigate the laboratory and construction performance of SFRPC.

According to the test results, when the fiber ratio exceeds 5 per cent, the concrete has difficulty meeting the workability requirements and this, therefore reduces the final strength and toughness. Therefore, only 5 per cent steel fiber was added to the RPC to improve its toughness. The steel fibers used were

made from cold drawn low-carbon steel. The fibers were 13 mm in length, 0.16 mm in diameter, and had a tensile strength in excess of 2000 MPa.

The cement used in this study was Jinning Rams 525# ordinary Portland cement which conforms to ASTM Type II standards. The selected dry silica fume had a specific gravity of 2100 kg/m<sup>3</sup> and an average particle size of 10<sup>-7</sup> m. Quartz sand produced in the Yangtze River was adopted in the tests. Additionally, a naphthalene-based superplasticizer was used to improve the slurry at low water-cement ratios.

The details of the mix proportions are listed in Table 1.

**Table 1. Concrete mix proportions**

Cement	Quartz sand	Quartz powder	Silica fume	Water-cement ratio
1.0	1.2	0.32	0.15	0.22

The compressive strength of the test samples prepared by extrusion (in the laboratory) was over 400 MPa. However, the mass SFRPC used for construction (cast-in-place and used in the following tests), has lower strength parameters in comparison. The specific gravity, compressive strength and dynamic fracture toughness of the tested SFRPC are 2850 kg/m<sup>3</sup>, 186 MPa, and 10.54 MPam<sup>1/2</sup>, respectively.

The water-cement ratio in the SFRPC is much lower than in ordinary concrete. The interface bond strength between the cement and steel fiber is, however, enhanced and thus the compressive strength and other strength parameters are greatly improved. The active powder used also upgrades the strength and toughness of the concrete by improving the interface bonding effect.

## 2.2 Test Procedure

### 2.2.1 Penetration Tests

The penetration test system consists of three parts: the launching system, the speed measurement equipment and the targets as shown in Fig. 1.

The launching system comprised a howitzer and corresponding projectiles as shown in Fig. 2. The speed measurement equipment included two frames covered by a conducting thin-wire mesh and one computer. When a projectile hit the mesh, the contact time was recorded by the computer. Thus, the velocity of the projectile was determined by dividing the distance between the two meshes by the recorded time interval. The projectiles used were made of

Chrome-Manganese-Silicon (*CrMnSi*) alloy steel, average Rockwell hardness of 49. The projectiles' parameters (body only, the empennage is not included) are listed in Table 2.

**Table 2. The parameters of projectiles**

	Weight (kg)	Diameter (mm)	Length (mm)
Group 1	2.32	57	138
Group 2	24.0	80	750

During the penetration tests, the projectiles were launched by the howitzer, passed the speed measurement equipments, and finally, hit the targets. After every hit, the penetration depth and crater area were checked and recorded for further analysis.

### 2.2.2 Contact Explosion Tests

The contact explosion tests were carried out in the blast test pit of PLA University of Science and Technology, China. In the tests, TNT solid explosive was directly placed on the SFRPC plates, on a flat clay foundation.

## 3. EXPERIMENTAL RESULTS

### 3.1 Penetration Tests

The penetration tests were divided into two groups depending on penetration speed.

The target used in the penetration tests are cylindrical, with an economical thickness pre-determined by analytical evaluation. The data recorded included the hit speed, penetration depth, and crater area.

#### 3.1.1 The First Group

The penetration speeds in the first group range from 308 m/s to 582 m/s and included ten SFRPC targets and no ordinary C30 concrete targets. The test data from the first group is given in Table 3.

Among the ten targets of the first group, only two targets (S1-2 and S1-10) were slightly damaged by cracks, except for the craters. On target S1-2, there were two apparent cracks with a maximum length of 25 cm and a maximum width of 5 mm, both cracks reached the side face of the target. On target S1-10, there was one 5 mm wide crack and the crack extended to the side face of the target. The other eight targets were intact, and only had a crater on the penetration side of each target.

The typical features in the targets of the first group after being hit are shown in Fig. 3. It appears that the projectile only

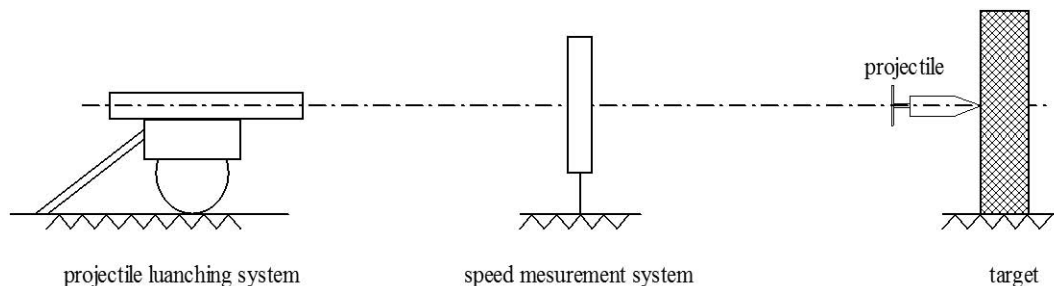


**Figure 1. The penetration test system.**



(a)



(b)



(c)



(d)

Figure 2. The launching system and the projectiles (a) 57 mm howitzer, (b) armor-piercing projectiles, (c) 125 mm howitzer, and (d) Earth penetrator model.

Table 3. Test results of the first group tests

No.	The size of target (cm)		Hit speed (m/s)	Penetration depth (cm)	Crater area (cm×cm)
	diameter	thickness			
S1-1	120	40	342	13.5	27×28
S1-2	120	40	582	21.0	45×39
S1-3	120	40	360	14.5	26×29
S1-4	120	40	410	17.8	28×28
S1-5	120	40	380	14.7	21×24
S1-6	120	20	328	12.5	21×28
S1-7	120	40	364	14.2	20×20
S1-8	120	40	550	19.7	70×65
S1-9	120	20	308	10.6	21×16
S1-10	120	20	364	14.0	22×24

made a small crater. In contrast, plain and ordinary reinforced concrete targets tend to break up because of radial cracks induced by the impact of the projectile.



Figure 3. Typical features of SFRPC targets after penetration (the first group).



3.1.2 The Second Group

The penetration speeds in the second group ranged from 808 m/s to 887 m/s and, included three SFRPC and three ordinary C30 concrete targets. The test data for the second group is listed in Table 4.

The three SFRPC targets in the second group remain intact, just like the majority of those in the first group. However, because the impact energy is much larger here than in the first group, the targets and projectiles were more seriously damaged. Thus the crater areas and the penetration depths were several times larger.

In contrast, the three ordinary C30 concrete targets were badly damaged by the projectiles. Target O-1 was penetrated to the backside and the other two targets were completely run through. All three targets had deep fissures on the side facing the impact and large areas peeling off from the backside.

Target O-1 after being hit is shown in Fig. 4. The picture was taken from the backside and the projectile is visible. The projectile's kinetic energy was exactly consumed when broke through the target.

Table 4. Test results of the second group

No.	The size of target(cm)		Hit speed (m/s)	Penetration depth (cm)	Crater area (cm×cm)
	diameter	thickness			
S2-1	160	200	852	133.0	66×59
S2-2	160	200	887	144.5	87×65
S2-3	160	200	847	132.5	63×51
O-1	160	360	808	360.0	150×120
O-2	160	360	880	Run through	130×115
O-3	160	360	836	Run through	74×65



Figure 4. Target No. O-1 after penetration.

3.1.3 Comparison with Analytical Evaluations of Ordinary Concrete

The study of penetration problems has a long history. A large number of experimental studies involving a wide

range of projectile sizes and impact velocities has provided several empirical or semi-empirical formulas for estimating penetration depth in rock-like materials. Good examples are such as the Young Formula, the Bernard Formulas, and the Berzai Formula.

Based on the theory presented by Wang<sup>9,10</sup>, calculation method of the penetration depth in SFRPC has been studied by Wang<sup>11</sup>, *et al.* who recommended the following formula:

$$h = \frac{M}{\rho d^2} \lambda_1 \lambda_2 K_p v \tag{1}$$

where  $h$  is the penetration depth,  $M$  is the mass of the projectile,  $d$  is the diameter of the projectile,  $v$  is the speed of projectile, and  $\lambda_1$ ,  $\lambda_2$ ,  $K_p$  are the shape factor, proportion scaling factor and the material penetration factor, respectively.

The shape factor  $\lambda_1$  reflects the influence of the length-diameter ratio of the projectile and can be expressed as

$$\lambda_1 = \frac{2\sqrt{1+4l_d^2/d^2}}{\pi(1+2\mu l_d/d)} \tag{2}$$

where  $\mu$  is the coefficient of sliding friction between the projectile and target, and  $l_d$  is the length of the warhead of the projectile.

The proportion scaling factor  $\lambda_2$  is deduced from the physical relationships of the cavity and crushing zone of the target material in the penetrating process. The expression for it is

$$\lambda_2 = \left\{ \frac{k}{k-1} \left[ \frac{1}{2} - \frac{4}{k+7} \left( \eta \sqrt{\frac{d}{2l_d}} \right)^{k-1} \right] \right\}^{-1} \tag{3}$$

where  $k$  and  $\eta$  are coefficients relating to the target material. For ordinary concrete, the material parameter  $k$  ranges from 1.6 to 1.8<sup>12</sup>. Here, for SFRPC targets,  $k = 2.0$ , and  $\eta = 0.46$ <sup>13</sup>.

The parameters ( $k$  and  $\eta$ ) in Eqn. (3) are empirically fitted by experimental data. The above parameter values are suitable for armour-piercing projectiles and middle to high speed penetration with an impact velocity ranges from 200 m/s to 1000 m/s.

The material penetration factor can expanded as

$$K_p = (\rho c_p)^{-1} \tag{4}$$

where  $\rho$  and  $c_p$  are the density and elastic wave velocity of the target material, respectively. The elastic wave velocity of the tested SFRPC is 1350 m/s.

In order to make a comparison between SFRPC and ordinary concrete, the penetration depths of the SFRPC targets (the first group) are plotted in Fig. 5, along with the results calculated using Eqn. (1) (for both SFRPC targets and ordinary concrete targets). In the calculations of the penetration depth in ordinary C30 concrete target, all the adopted projectile parameters are identical to those used in the tests.

The test results show that the anti-penetration capability of the SFRPC targets is far superior to ordinary C30 concrete targets. The penetration depth in SFRPC targets are about half the theoretical evaluated depths in ordinary C30 concrete targets when the penetration speed ranges from 300 m/s to 600 m/s. The comparison between the test data and theoretical evaluation of the penetration depth in SFRPC targets indicates

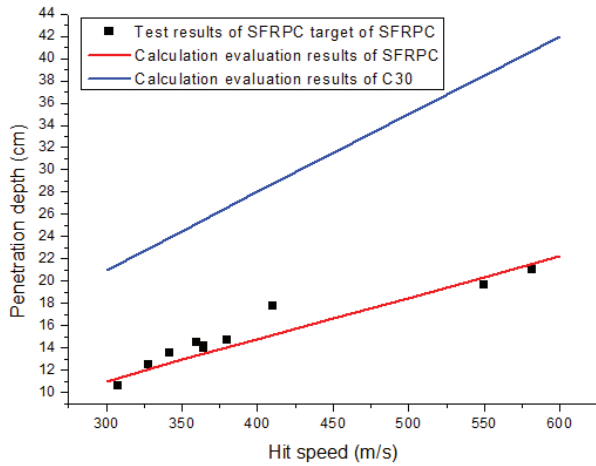


**Figure 5. Comparison between test data and theoretical evaluation of penetration depth.**

that the theoretical evaluation method recommended by Wang is reliable.

When the penetration speed is higher than 800 m/s, the SFRPC targets show even better anti-penetration capability. From Table 4, the penetration depths in ordinary C30 concrete targets are larger than the thickness of the target. The conservatively estimated penetration depth in ordinary C30 is two times larger than the penetration depth in SFRPC targets under similar conditions.

### 3.2 Contact Explosion Tests

In the contact explosion tests, the explosive was detonated, acted upon the SFRPC plates, and made an explosion funnel to a certain depth (explosion cavity radius). The depths and areas of the explosion funnels were recorded after every test.

#### 3.2.1 Test Results

The parameters of the SFRPC test plates and the recorded results are listed in Table 5.

All the tested SFRPC plates remained intact, except for

**Table 5. Targets' characters and the test results of contact explosion**

No.	Thickness (cm)	Explosive charge (kg)	Explosion funnel	
			Depth (cm)	Area (cm <sup>2</sup> )
S3-1	20	0.5	3.2	6×7
S3-2	20	0.5	3.4	6×7
S3-3	20	1.0	4.0	9×11
S3-4	20	1.0	4.1	7×10
S3-5	30	1.5	4.7	13×14
S3-6	30	1.5	4.6	14×14
S3-7	30	2.0	4.9	16×16
S3-8	30	2.0	5.2	17×17
S3-9	30	2.5	5.9	16×17
S3-10	30	3.0	6.6	21×22
S3-11	30	3.0	6.7	23×23

the explosion funnel.

The explosion funnels were made by the direct action of detonation waves at high temperature and high pressure. The areas and depths of the explosion funnels are determined by many factors which can be classified as follows. First-class factors are the properties of the charge, including the charge shape, density, and detonation velocity. Second-class factors are the parameters of the target plates, such as thickness, strength, density, and steel fiber content. Third-class factors are the boundary conditions and the mode of interaction.

In each contact explosion test, the explosive type, the boundary conditions and the mode of interaction were all identical. Therefore, the differences in the explosion funnels resulted from differences in the charges and the parameters of the target.

#### 3.2.2 Comparison with Ordinary Concrete

According to an early investigation by Wang<sup>14</sup>, the explosion cavity radius can be calculated from the following formula:

$$r_a = K_a \sqrt[3]{W} \quad (5)$$

where  $r_a$  is the explosion cavity radius,  $K_a$  is the compression coefficient of the material, and  $W$  is the mass of the effective charge.

By fitting the explosion cavity radius data listed in Table 5, the compression coefficient of SFRPC thus be obtained, with the result that  $K_a = 0.042$ . The test results and the fitted explosion cavity radii (vs. the mass of the charge) are shown in Fig. 6.

In order to make a comparison, the explosion cavity radii of ordinary C30 concrete targets were also calculated using Eqn. (5). According to Qian & Wang<sup>12</sup>, the compression coefficient is 0.17. A comparison is shown in Fig. 6, it is seen that the explosion cavity radii in the ordinary C30 concrete targets are about four times those in the SFRPC targets. In other words, the anti-explosion capability of SFRPC is about three times higher than that of ordinary C30 concrete targets.

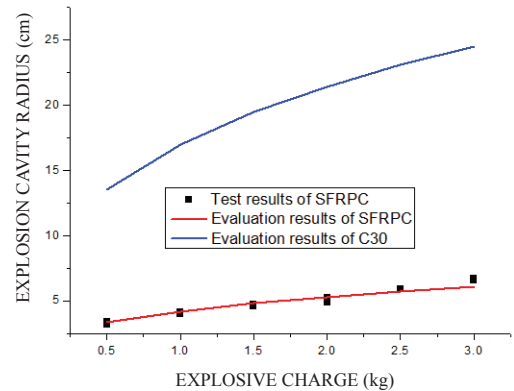


**Figure 6. Comparison between the explosion cavity radius of SFRPC and ordinary C30 concrete.**

## 4. CONCLUSIONS

A series of tests were carried out to investigate the anti-penetration and anti-explosion capability of steel-fiber reactive powder concrete. From an analysis of the tests results, the following conclusions can be drawn:

- (a) The anti-penetration capability of the tested RPC with 5% steel fiber is significantly better than that of ordinary concrete. The tested penetration depths of SFRPC targets are smaller than one half of the corresponding value in ordinary C30 concrete.
- (b) A theoretical evaluations of a formula recommended by Wang D R for calculating penetration depths in SFRPC coincide well with the experimental observations from the penetration tests.
- (c) The anti-explosion capability of SFRPC is about four times better than that of ordinary C30 concrete.

In summary, the anti-strike capability of RPC with 5 per cent steel fiber is markedly superior to ordinary concrete. Meanwhile, the tested SFRPC met the workable performance requirement for construction. In conclusion, SFRPC is a commendable material for protective structures.

## 5. ACKNOWLEDGEMENT

The authors gratefully acknowledge the financial support from the National Science Fund for Distinguished Young Scholars (Grant: 50825403) and the Science Fund for Creative Research Group of the NSFC (Grant: 510210001).

## REFERENCES

1. Abid, A.S. & Ribakov, Y. Recent trends in steel fibered high-strength concrete. *Mater. Design*, 2011, **32**(8), 4122-4151.
2. Zhang, Yunsheng; Sun, Wei; Liu, Sifeng; Jiao, Chujie & Lai, Jianzhong. Preparation of C200 green reactive powder concrete and its static-dynamic behaviors. *Cement Concrete Comp.*, 2008, **30**(9), 831-838.
3. Cwirzen, A.; Penttala, V. & Ornanen, C.V. Reactive powder based concretes: Mechanical properties, durability and hybrid use with OPC. *Cement Concrete Res.*, 2008, **38**(10), 1217-1226.
4. Wang, Yonghua; Wang, Zhengdao; Liang, Xiaoyan & Minzhe, An. Experimental and numerical Studies on dynamic compressive behavior of reactive powder concretes. *Acta Mech. Solida Sin.*, 2008, **21**(5), 420-520.
5. Lai, Jianzhong; Sun, Wei & Liu, Sifeng. Effect of steel fiber on improving compressive strength of RPC. *Chin. Concrete Cement Prod.*, 2002, **21**(5), 41-43.
6. Taia, Yuh-Shiou; Panb, Huang-Hsing & Kung, Ying-Nien. Mechanical properties of steel fiber reinforced reactive powder concrete following exposure to high temperature reaching 800 °C. *Nucl. Eng. Des.*, 2011, **241**(7), 2416-2424.
7. Ju, Yang; Liu, HongBin; Sheng, GuoHua & Wang, HuiJie. Experimental study of dynamic mechanical properties of reactive powder concrete under high-strain-rate impacts. *Sci. China Tech. Sci.*, 2010, **53**(9), 2435-2449.
8. Zhimin, Tian; Huajie, Wu; Xiquan, Jiang; Yan, Peiyu & Jianwen, Feng. Ultra high performance concrete RPC under compressive impact loading. *J. PLA Univ. Sci. Tech.*, 2007, **8**(5), 463-469.
9. Wang, Mingyang, Zheng, Daliang & Qian, Qihu. The scaling problems of penetration and perforation for projectile into concrete media. *Explo. Shock Waves*, 2004, **24**(2), 108-114.
10. Qian, Qihu & Wang, Mingyang. Impact and explosion effects in rocks and soils. National Defense Industry Press, Beijing, 2010.
11. Wang, Derong; Ge, Tao & Zhou zeping. Investigation of calculation method for anti-penetration of reactive power steel fiber concrete (RPC). *Explo. Shock Waves*, 2006, **26**(4), 367-372.
12. Qian, Qihu & Wang, Mingyang. Calculation theory for advanced protective structure. Nanjing: Phoenix Publishing, 2009 (Chinese).
13. Wang, Mingyang & Wang, Derong. Practicable design method for reactive powder steel fiber concrete under local damage loads. PLA Univ. Sci. Tech., Nanjing, National Defence Science and Technology Report. 2006.
14. Wang, Derong; Dai, Ming; Li, Jie & Wang, Mingyang. Failure effect of steel-fiber reactive power concrete (RPC) shelter plate under contact explosion. *Explo. Shock Waves*, 2008, **28**(1), 67-74.

## Contributors



**Dr Fan P.X.** obtain his Masters degree (Civil Engg) and PhD (Civil Engg) from PLA University of Science and Technology, in 2007 and 2011. Presently he is working as post-doctoral research fellow in College of Field Engineering, PLA University of Science and Technology. His areas of interest include: underground protective structure, rock mechanics, anti-penetration material, and geomechanics model test.

**Dr Wang M.Y.** obtain his PhD (Civil Engg) from PLA University of Science and Technology in 1994. Presently he is working as Director of State Key Laboratory of Disaster Prevention & Mitigation of Explosion & Impact, PLA University of Science and Technology. His areas of interest include: protective structure, high performance material, rock mechanics, structural dynamics.



**Dr Song C.M.** obtain his Masters degree (Civil Engg) and PhD (Civil Engg) from PLA University of Science and Technology, in 2005 and 2008. Presently he is working as Lecturer at State Key Laboratory of Disaster Prevention & Mitigation of Explosion & Impact, PLA University of Science and Technology. His areas of interest include: Protective structure, structural dynamics.